SCANNING VOL. 20, 302–310 (1998)

Received April 6, 1998
Accepted April 24, 1998

Correlating Auger Electron Spectroscopy with Scanning Electron Microscopy-Energy Dispersive Spectroscopy for the Analysis of Respirable Particles

JAMES W. STEPHENS, JOEL C. HARRISON, WILLIAM E. WALLACE

Health Effects Laboratory Division, National Institute for Occupational Safety and Health, Morgantown, West Virginia, USA

Summary: A method has been developed to characterize large populations of individual respirable particles. With the use of custom data collection and data correlation computer software, the same set of particles can be analyzed in multiple instruments. The method is demonstrated by the analysis of a sample of hard-metal particles. A series of particles are analyzed by Auger electron spectroscopy, and then the same particles are analyzed by scanning electron microscopy-energy dispersive spectroscopy.

Key words: Auger electron spectroscopy, scanning electron microscopy, hard-metal, data analysis, respirable particles

Introduction

Workplace exposure to respirable particles is known to be a serious occupational hazard in many industries. Unfortunately, the chemical and physical characterization of these particles is notoriously difficult (Jambers *et al.* 1995, Van Grieken and Xhoffer 1992). Many of the most commonly used analysis methods, such as infrared spectroscopy or x-ray diffraction, only provide bulk properties of the sample. While this may be sufficient for homogeneous exposures, for heterogeneous exposures, or when looking for trace contaminants in homogeneous samples, particle-by-particle analysis is often needed for the separate characterization of the individual contributions which make up the total exposure (Cornille *et al.* 1990, De Bock *et al.* 1994, Michaud *et al.* 1996). Moreover, the particles themselves may not be homogeneous—for example, they may have surface coatings (Wallace *et al.* 1990) or they may be aggregates of smaller particles—so that an entire vector of data may be needed for each particle to characterize the exposure fully.

Unfortunately, the small size of respirable particles severely limits the analytical techniques available for particle-by-particle analysis. Ideally, such a technique should provide both morphologic and compositional information about each particle with submicrometer resolution; and in many cases, the technique must be able to provide this information for hundreds or thousands of particles per sample to satisfy the statistical demands of a study.

The scanning electron microscope equipped with an energy dispersive spectrometer (SEM-EDS) has become a workhorse in the area of respirable particulate identification and analysis (e.g., Abraham and Hunt 1995, Fruhstorfer and Niessner 1994, Van Grieken and Xhoffer 1992, Wallace *et al.* 1996, Xhoffer *et al.* 1991). The combination of the high spatial resolution of SEM combined with the sensitivity of EDS provides a powerful tool for elemental analysis of small particles. In addition, modern SEM systems often provide the ability to perform automated analysis of multiple fields of particles, making it practical to analyze hundreds or thousands of particles per sample.

In the SEM-EDS technique, the analysis volume typically extends some tens of micrometers into the sample. For particles in the micrometer size range, this means that the analysis volume extends all the way through the particle. In contrast, the analysis volume in Auger electron spectroscopy (AES) is normally on the order of only a few atomic layers deep. Therefore, AES is often used as a complementary technique to SEM-EDS. The electron beam in most AES systems can be scanned across the sample, providing imaging capabilities similar to an SEM. Thus, a combination of SEM-EDS and AES measurements provides elemental information of both the entire particle, as well as surface specific information.

Scanning electron micrscopy-energy dispersive spectroscopy has often been used in conjunction with AES and other surface analysis techniques for analysis of particulate samples (Childs *et al.* 1996, Grekula *et al.* 1986, Michaud *et al.* 1996). Attempts to use these two techniques together in an integrated fashion have not been common because most instruments do not have both the electron energy analyzer needed for AES along with the x-ray detector needed for SEM-EDS. Although measurements using both techniques are often performed on particulate samples, the identities of the specific particles usually are lost as the samples are moved from one instrument to another. Uritsky *et al.* (1997) describe

Address for reprints:

James W. Stephens
NIOSH
1095 Willowdale Rd.
Morgantown, WV 26505, USA

the use of a commercial laser-based particle mapping system to re-find small particles for analysis by both SEM-EDS and AES. However, in their studies AES measurements were only performed on a small number of particles, and their technique requires the use of additional expensive equipment. In general, correlated SEM-EDS and AES measurements have not been made on large numbers of particles.

In the studies detailed herein, a method has been developed to analyze large numbers of particles using both SEM-EDS and AES, preserving the particle identities in the process. In many cases, this method can be applied to existing equipment without hardware modification. A combination of custom and commercial data collection software has been used for automated particle analysis, followed by a postprocessing phase which correlates the acquired data and removes false-positive analysis points. This method is generally effective enough to be readily adapted for use with other types of instruments, such as confocal microscopes, atomic force microscopes, or Raman microscopes.

Experimental

Particle analysis using a respirable dust sample consisting of overspray from a hard-metal detonation gun is demonstrated. A few micrograms of this sample were suspended in isopropyl alcohol, and several drops of the suspension were allowed to evaporate on a 1 cm diameter carbon planchette. Four X marks and one additional index mark were made on each planchette using a razor blade. The X marks served as registration points used in setting the coordinate system for the sample (vide infra). The lone index mark was used to establish unambiguously the orientation of the registration marks (Fig. 1).

The AES measurements were made on a Physical Electronics 5700 Multitechnique system equipped with a model 10-210 electron gun, an Omni Focus V lens, a model 10-360 spherical capacitor analyzer, a multiple channel detector, and PC-Access data collection software (version 6.0F). The sample was cleaned with a brief (60 s) Ar ion sputter prior to analysis to remove residue from the solvent. Secondary electron images and Auger spectra were collected using an electron accelerating voltage of 3 keV and an image magnification of 700×. To achieve maximum electron flux to the sample, the condenser lens was opened to the point where the smaller particles could still just be resolved. The electron beam current measured at the sample was ~10 nA. Survey spectra were taken of each particle at a 1 eV resolution, 20 ms per point, with 20 sweeps averaged to produce each spectrum. The electron energy analyzer was operated in fixed retard ratio mode with $\Delta E/E = 0.6\%$. The AES peak heights were determined after subtracting a cubic background fitted to the baseline on either side of the peak and then converted to equivalent peak-to-peak values so that concentration could be determined using published sensitivities (Physical Electronics 1996).

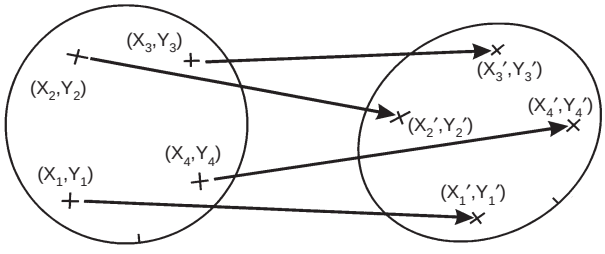

FIG. 1 Schematic diagram of a carbon planchette as viewed in two different instruments. Registration marks (Xs) have been added with a razor blade. By using the coordinates of the registration marks, a transformation can be found to convert the coordinates on the left to those on the right.

Scanning electron microscopy-energy dispersive spectroscopy measurements were made using a Jeol JSM-6400 microscope with a Princeton Gamma Tech model OPJ0411243 detector equipped with an Omega ultra-thin window. X-ray spectra were collected at 20 kV accelerating voltage. The secondary electron image of each field of particles was collected at 700× magnification. X-ray spectra were collected for each particle in the field for 30 s (live time) per analysis point, with a detector dead time of ~25%. Electron beam current was ~500 pA.

New Method

Current commercial SEM software and hardware allow for easy imaging of multiple fields of particles, with the subsequent analysis of each particle from x-ray spectra acquired by EDS. The difficulty comes in attempting to analyze the same particles in different instruments. For this study, the hard-metal samples were to be analyzed by EDS to determine the total composition of each particle, and then the same particles were to be analyzed in an AES spectrometer to determine the surface composition. It was desirable to be able to analyze a large number of particles (in the hundreds per sample) using each technique, so finding the particles manually for the second and subsequent runs was not considered practical.

When multiple fields of particles must be analyzed, the problem of finding the particles is two-fold. First, the original field of particles must be found on the planchette; second, the identical particles analyzed in this field during the first experimental pass must be found so that they may be analyzed a second time under the new conditions. In addition, if one wishes to collect images under the two conditions so that the images can be compared (or published) side by side, a third requirement may arise; the two images may need to be transformed so that they occupy the same coordinate space.

The three problems above can be generalized to one of transforming one coordinate space into a different coordi-

nate space. For example, the stage coordinates of the fields on the planchette, when measured in the first instrument, must be transformed to a new set of coordinates when the sample is put into the second instrument so that the fields can be relocated. Since the sample may be rotated or shifted when moved from one stage to another, and the scales of the two stages may not be identical, it is easiest to transform the coordinates using a 2×2 transformation matrix followed by a translation vector.

$$\begin{pmatrix} x' \\ y' \end{pmatrix} = \begin{bmatrix} t_{11} & t_{12} \\ t_{21} & t_{22} \end{bmatrix} \begin{pmatrix} x \\ y \end{pmatrix} + \begin{pmatrix} x_{offset} \\ y_{offset} \end{pmatrix}$$

Once the field has be found and imaged a second time, a second transformation is needed to convert the pixel coordinates of the first image into the pixel coordinates of the second image. Using these coordinates, the images can be overlaid to locate identical particles or for other comparisons. Once again, if the imaging is linear and the samples are sufficiently flat, the image from one instrument can be converted to the coordinate system of the image from the second instrument by a 2×2 matrix transformation followed by a translation vector.

In the method detailed here, the first transformation was determined with the aid of four small Xs which were scratched into the sample planchette with a razor blade. During the analysis in the AES system, the stage coordinates necessary to bring the center of each X into the center of the field of view were recorded, along with the stage coordinates of each analysis field. Then, when the sample was moved to the SEM, the new stage coordinates of the four registration Xs were determined and the transformation parameters were calculated using a least-squares fit. These parameters were then used to predict the SEM stage locations of the analysis fields (Fig. 1).

Once a field was relocated, analysis points within each field were determined separately for each instrument based on the newly collected images. For the SEM measurements, a binary threshholding algorithm was applied to the secondary electron image and the binary features were assumed to be particles to be analyzed. Analysis points were selected manually in the AES instrument because shadowing problems in the secondary image made threshholding difficult.

Since the particle identification processes are performed independently in each of the two instruments, it is still necessary to identify the analysis points which correspond to identical particles between runs. The approach chosen here was to write additional software which guides the user through the task of aligning the images (and therefore the analysis points) to one another. The user selects several points on the screen which are common between the two images. A least-squares fit then determines the best transformation parameters to map the identical points to one another. Once this mapping has been accomplished, the software searches for analysis points from different runs which lie within a proscribed distance to one another. All measurements which can be so correlated are saved to a spreadsheet file, and the uncorrelated points which remain are discarded. Since the entire correlation process can be performed in less than a minute per field of particles, the technique is appropriate for very large numbers of measurements. Furthermore, sufficient data are archived to allow backtracing of any data point all the way back to finding the original particle on the planchette.

The parameters used to transform the particle coordinates can also be used to transform the images as well. This allows the images to be presented on the same scale and orientation for easy comparison or for publication. Software was written in Perl 5.003 to transform an image using the transformation parameters calculated from the least-squares procedure.

Custom computer software was written to save all of the data necessary to recreate the field positions and the analysis points in each field. For the SEM-EDS analysis, scripts were written to interface with the Princeton Gamma Tech IMIX software version 8.288. These scripts automate the microscope to move the sample stage to a new field, collect a secondary electron image of the new field, and then analyze each of the particles in the field with EDS. For each field, the software saves the coordinates of the field on the stub, the secondary electron image, the position of each analysis point within the field, morphologic information about each particle, and the x-ray spectrum for each particle.

Additional custom software was written to serve as a front end program to the PC-Access software. A front end interface was needed to provide data archiving and image analysis for each analysis field and to overcome some limitations of the commercial software (most notably, a limit of 20 analysis points per sample run). Using the front-end software, an image is collected and data points are selected either manually or as the result of an image analysis algorithm. The data points are then collected in batches of 20 or fewer. Coordinate data are saved so that the analysis points can be superimposed on image at a later date. The sample stage is then adjusted manually to move to the next field of particles.

Results and Discussion

Four fields of particles were analyzed by both AES and SEM-EDS to simulate the analysis of a real-world sample. During the AES data collection, 266 analysis points were selected manually over the four fields. The AES data collection proceeded at ~10 particles/h, so each field could be analyzed during an overnight run. When the same fields were analyzed in the SEM, the automatic threshholding routine identified somewhat more points (521) for further analysis. However, due to the faster collection time in the SEM, all four fields were analyzed in a single 6 h run. The resulting data files were fed through the correlation software where 252 correlated pairs were identified. Although 95% of the AES particles found matches in the SEM-EDS data, only 48% of the SEM particles found AES matches. This is due,

in large part, to the fact that SEM fields were larger than those on the AES; approximately 30% of the particles analyzed by SEM-EDS were outside the boundaries of the fields collected in the AES instrument. In addition, the image resolution was better in the SEM, so some of the smallest particles were missed in the images from the AES instrument.

The processing of a single field of measurements is illustrated in Figures 2–5. Figure 2a and b shows the original images as collected in each instrument. In Figure 3a and b, the data files from the data collection software have been used to recreate the data collection process. The correlation program has been used to display the images and label each analysis point. The X marks are locations selected by the user indicating identical spots on each image. The software then uses the X marks to determine the transformation parameters necessary to map one image into another. In Figure 4, these transformations have been applied to the AES image to deform it into the same coordinate space as the SEM image (compare Fig. 4 with Fig. 2b). The data correlation software also transforms the coordinates of the AES analysis points by the same method and overlays the transformed points on top of the SEM points for correlation, as shown in Figure 5.

Figure 6a shows an expanded view of the bottom center region of Figure 2b. Both SEM-EDS and AES spectra are shown in Figure 6b for each of the three labeled particles. Although the particles B and C both appear to be high tung-

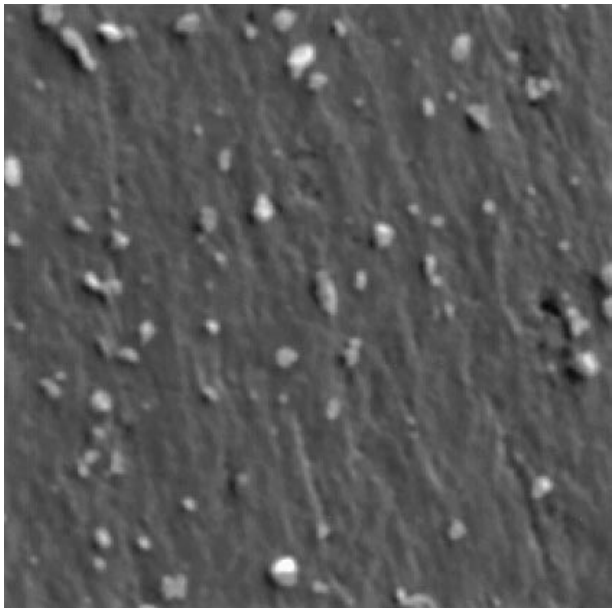

(a)

(b)

FIG. 2 Secondary electron images of a typical field of hard-metal particles. (a) Image from AES instrument; horizontal field width = 140 µm. (b) Image from SEM instrument; horizontal field width = 165 µm.

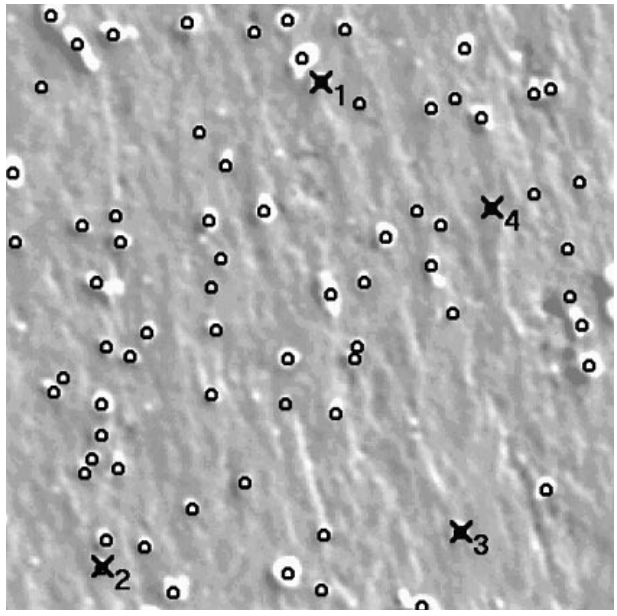

(a)

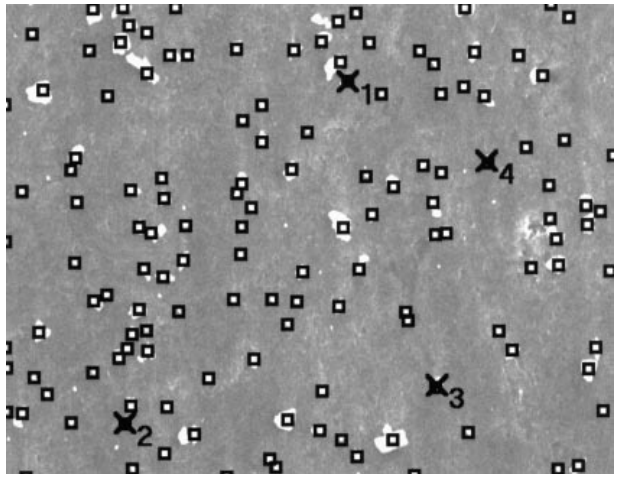

(b)

FIG. 3 Points analyzed using (a) AES and (b) SEM-EDS, as displayed by the data correlation software. Circles are AES analysis locations, and squares are SEM-EDS analysis locations. The user has selected four locations on each image which correspond to identical points (xs).

sten particles with similar compositions when probed with SEM-EDS, the Auger spectra reveal that particle C has considerably more chromium and cobalt on the surface than particle B. Particle A has cobalt both on the surface and throughout the particle.

One strength of making correlated measurements is the ability to identify properties of particles in various subpopulations of a sample. For example, the particles analyzed for the current study are plotted in Figure 7a according to their estimated concentrations of tungsten, cobalt, and chromium (the predominate metals found for this sample) as determined by SEM-EDS. Because of the difficulties associated with quantitative analysis of small particles, only approximate elemental concentrations were calculated using a standardless k-ratio method. Particles with low SEM-EDS signals (<1000 counts) for the three primary elements were left out of the diagram. Based on these data, the particles were then (somewhat arbitrarily) classified into four categories according to SEM-EDS composition. These categories are labeled in Figure 7a as (b) high tungsten, (c) tungsten with some cobalt (<20%), (d) tungsten with higher amounts of cobalt (>20%), and (e) tungsten with chromium.

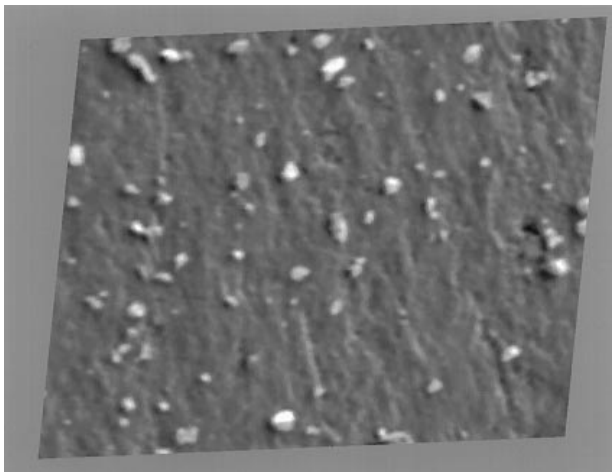

FIG. 4 The AES image from Figure 2a after transformation into the coordinate space of Figure 2b. The transformation parameters were determined by the software using the xs in Figure 3.

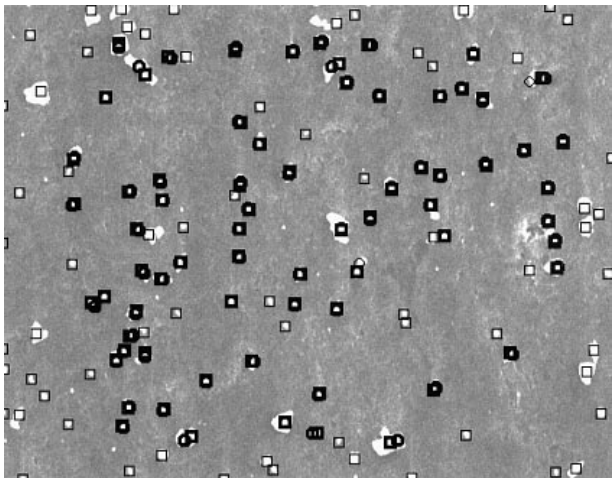

FIG. 5 The AES analysis points from Figure 3, transformed to the SEM coordinate space and overlayed on top of the SEM image and analysis points. Bold points are those which have been identified by the software as correlated pairs.

The surface compositions, as determined by AES, were then examined for each category. Figure 7b through e shows the surface (AES) data for categories b through e (as labeled in Fig. 7a), respectively. For example, Figure 7b displays the surface compositions of the particles determined to be high in tungsten (category b in Fig. 7a) from the SEM-EDS data.

From the correlated data, the following conclusions can be drawn: (1) Particles with bulk cobalt concentrations also show surface cobalt (Fig. 7c and d); (2) particles with bulk chromium concentrations also show surface chromium (Fig. 7e); (3) some particles which look like pure tungsten in the bulk analysis look like pure tungsten in the surface analysis, but others show significant amounts of cobalt and chromium (Fig. 7b). Thus it appears that some of the particles are tungsten with a thin coating of cobalt or chromium on the surface.

In the results presented here, it was relatively easy to identify the particles because the large differences in density between the hard-metal sample particles and the carbon substrate produce high contrast SEM images. Moreover, the particles were identified manually for AES analysis, further reducing the number of false identifications. However, for other types of samples, the number of incorrect particle identifications may be much greater. Obviously, if a reliable analysis method is desired, particle identification criteria which consistently identify the same particles are desired.

The above problem is not as serious as it might appear initially. It is generally advisable to set the particle identification parameters on the generous side so that there are false-positive identifications rather than false negatives. Since the human eye is generally more reliable than computer algorithms at identifying particles in an image, the interactive data correlation software is designed to allow the user to override quickly the false-positive identifications with a mouse click. Although the same effect could be achieved by requiring a human operator to be present to identify the particles during the data collection step, it is much faster and more efficient to collect some number of false-positive points and then remove them during the postprocessing phase.

Furthermore, it is frequently unnecessary to remove the false-positive points at all. Since the particle identification processes are performed on images collected under different conditions, the false-positive points are rarely the same on each image. Therefore, the act of correlating the measurements often removes many or all of the false-positive points. In test runs using lower density mineral particles (which produce lower contrast images), it was found that most of the false-positive measurements were due to substrate texture and imperfections. Since these imperfections

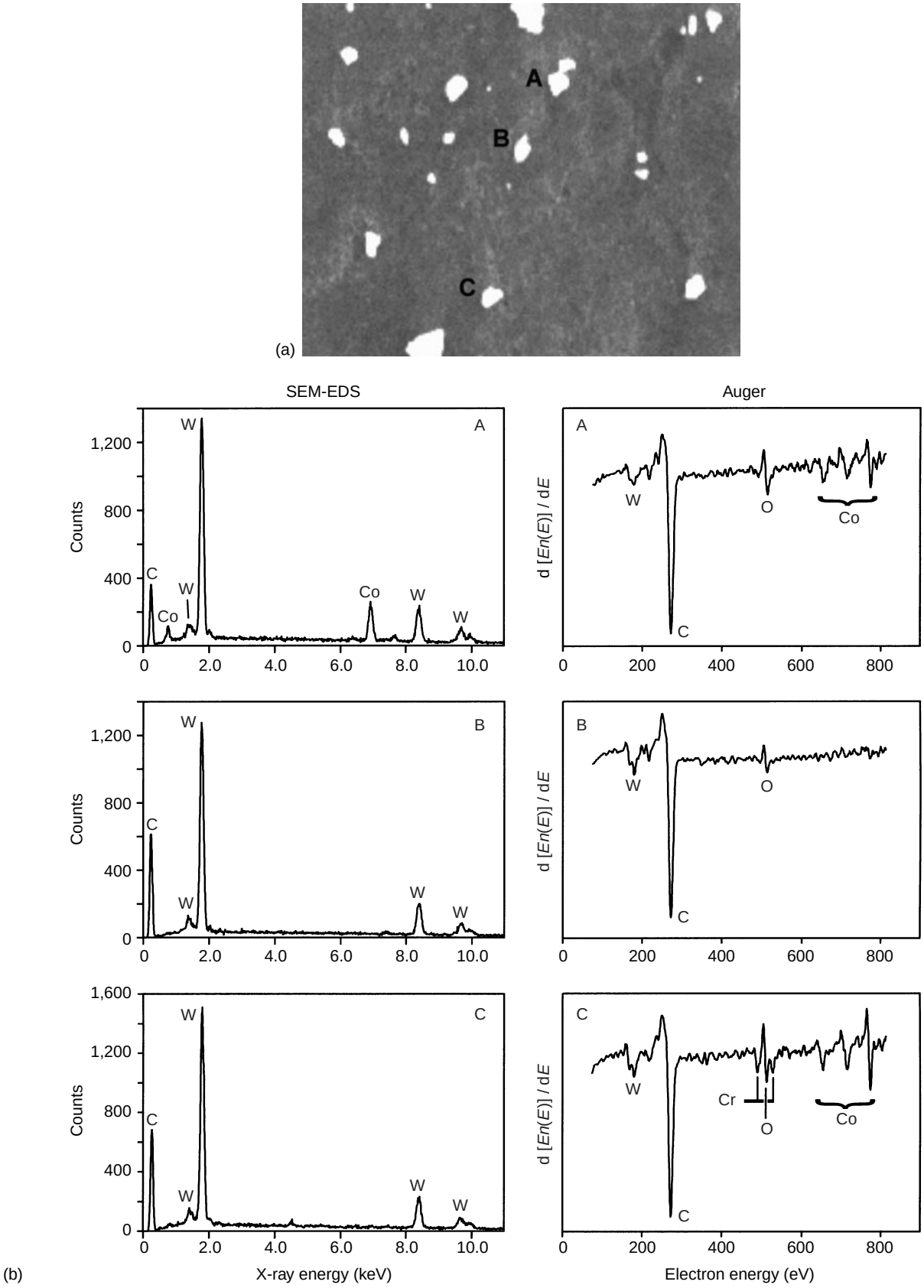

FIG. 6 Sample spectra for three particles. (a) Expanded view of the bottom center portion of Figure 2b; (b) SEM-EDS and AES spectra for the three labeled particles.

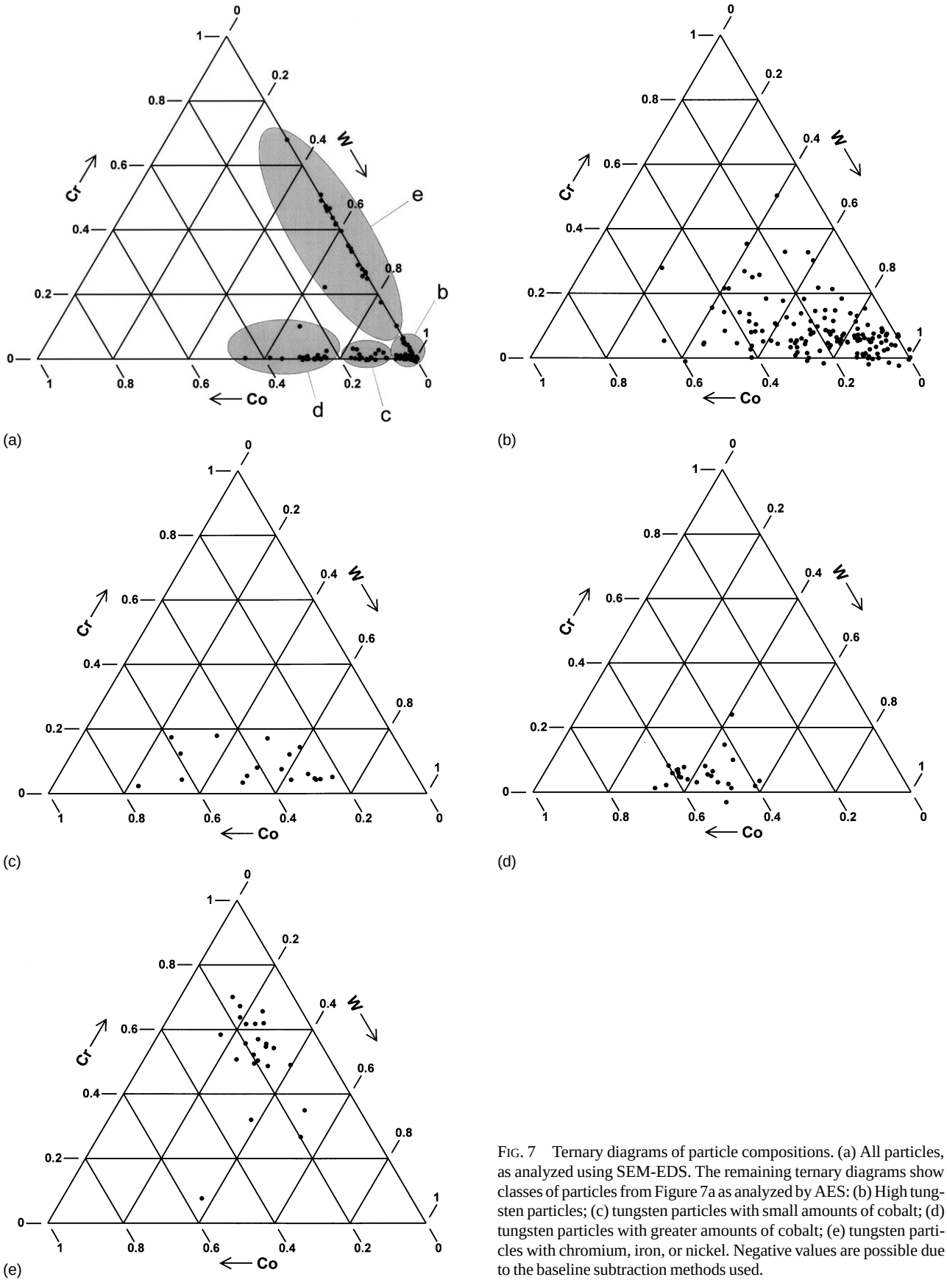

FIG. 7 Ternary diagrams of particle compositions. (a) All particles, as analyzed using SEM-EDS. The remaining ternary diagrams show classes of particles from Figure 7a as analyzed by AES: (b) High tungsten particles; (c) tungsten particles with small amounts of cobalt; (d) tungsten particles with greater amounts of cobalt; (e) tungsten particles with chromium, iron, or nickel. Negative values are possible due to the baseline subtraction methods used.

varied in appearance in the two instruments, the false positives generally did not find a mate when the data were correlated. This also highlights the importance of setting the particle identification parameters too generously; a lone false-positive point will often be removed when the data are correlated, but a missed point (false-negative) will result in the entire particle being dropped from the data set.

It proved to be difficult to collect the same quantity of AES data as SEM-EDS data. Much longer collection times are needed for AES to achieve the same signal-to-noise ratio as can be achieved with SEM-EDS. Furthermore the AES instrument used in this work was an x-ray photoelectron spectrometer outfitted with an electron gun. In this instrument, the gun is placed at an angle from the sample, so the images always showed heavy shading on one side of the particles. This made the automated identification of the particles less reliable, so manual identification was used. Since the data collection time for the AES fields was typically on the order of several hours, it was practical to select manually the analysis points at the beginning of the (usually overnight) run without slowing down the data collection.

The angle of the electron beam also meant that the secondary electron image collected on the AES instrument was deformed compared with the image collected on the SEM. As detailed above, for a two-dimensional sample this deformation can be represented by a 2×2 matrix transformation matrix followed by an x and y offset. For a flat stub with small three-dimensional particles, this transformation is still a good approximation of the actual image deformation. However, there may still be a noticeable difference in the two images in areas where large particles protrude above the surface. In practice, this is not a serious problem for respirable particles. When selecting identical reference points on the images, it is best to use small particles which will appear similar from any orientation. If analysis is desired of larger particles, which are frequently not in the respirable size range anyway, the analysis points can be manually correlated using the custom software interface.

One significant problem with our approach to multiple-instrument particle analysis is that the different instruments will likely sample slightly different spots on the particles. The thresholding process generates slightly different particle shapes and sizes on each instrument, thus the particle center will be assigned to a slightly different point in each instrument. Moreover, since the viewpoint of the image is from an angle in the AES instrument, the perceived center of the particle is not the same as when it is viewed from above, as in the SEM instrument.

The error introduced by these effects is not judged to be important for the small (<1 μm diameter) particles; for these particles the analysis points appear to be very close for the two techniques. However, for large particles, especially >5 μm in diameter, the analysis points may be in significantly different positions, sometimes far enough apart that the software does not correlate them automatically. When such an event occurs, they can be correlated manually, but if the particle is sufficiently heterogeneous the points may be sampling different environments on the particle. One possible solution to this problem is to modify the SEM-EDS data collection software to collect a small grid of points, instead of a single point, for sufficiently large particles. Then, it is hoped, at least one of these grid points would fall close enough to AES analysis point to make a valid correlation between the two measurements. (Naturally, the remaining grid points would automatically be discarded when the data are correlated.) This approach has not been tried.

Although the studies detailed here have used an SEM and an AES/XPS instrument, the techniques are broadly applicable to a variety of instruments. For example, Raman microscopy could be combined with SEM-EDS using these methods to provide correlated chemical and elemental information about particles, or elemental analysis of particles in tissue could be combined with confocal microscope fluorescence data of the same particles. Because these techniques rely heavily on postprocessing of the data, it is not necessary to combine these techniques in a single instrument; existing equipment can be used, even if located at different facilities. Moreover, the automated data collection capabilities of a wide variety of instruments can be exploited.

The technique presented here is referred to as being for multiple instruments, but it is just as applicable for measurements made under two different conditions or at two different times in the same instrument. For example, a method has been developed to depth-profile surface-occluded silica particles using SEM-EDS at two or more accelerating voltages (Wallace and Keane 1993). Although the measurements at the various voltages can be made without removing the sample from the instrument, there is generally a shift in the image when the voltage is changed, so the same analysis points cannot be reused. The postprocessing data correlation method has been successfully used for two-voltage depth profiling, with a throughput of up to 500 particles in 24 h.

Conclusion

Correlated SEM-EDS and AES measurements of large numbers of individual, respirable-sized particles are made practical by the use of a postprocessing data correlation method coupled with custom data collection software. The data are collected under computer automation, allowing unsupervised or overnight data acquisition. Custom data correlation and analysis software is used for quick correlation and display of the resulting data. Any data point in the processed data can be easily traced back to the original measurements. It is even possible to relocate the particle on the planchette for additional measurements, if so desired.

References

Abraham JL, Hunt A: Environmental contamination by cobalt in the vicinity of a cemented tungsten carbide tool grinding plant. *Environ Res* 69, 67–74 (1995)

Childs KD, Narum D, LaVanier LA, Lindley PM, Schueler BW, Mulholland G, Diebold AC: Comparison of submicron particle analysis by Auger electron spectroscopy, time-of-flight secondary ion mass spectrometry, and secondary electron microscopy with energy dispersive x-ray spectroscopy. *J Vac Sci Technol A* 14, 2392–2404 (1996)

Cornille P, Maenhaut W, Pacyna JM: Sources and characteristics of the atmospheric aerosol near Damascus, Syria. *Atmospheric Environ* 24, 1083–1093 (1990)

De Bock LA, Van Malderen H, Van Grieken RE: Individual aerosol particle composition variations in air masses crossing the North Sea. *Environ Sci Technol* 28, 1513–1520 (1994)

Fruhstorfer P, Niessner R: Identification and classification of airborne soot particles using an automated SEM/EDX. *Mikrochim Acta* 113, 239–250 (1994)

Grekula A, Ristolainen E, Tanninen VP, Hyvärinen HK, Kalliomäki PL: Surface and bulk chemical analysis on metal aerosols generated by manual metal arc welding of stainless steel. *J Aerosol Sci* 17, 1–9 (1986)

Jambers W, De Bock L, Van Grieken R: Recent advances in the analysis of individual environmental particles. *Analyst* 120, 681–692 (1995)

Michaud D, Baril M, Dion C, Perrault G: Characterization of airborne dust from two nonferrous foundries by physico-chemical methods and multivariate statistical analyses. *J Air & Waste Manage Assoc* 46, 450-457 (1996)

Physical Electronics: *MultiPak Ver. 2.2 Operator's Manual* (1996)

Uritsky Y, Chen L, Zhang S, Wilson S, Mak A, Brundle CR: Root cause determination of particle contamination in the tungsten etch back process. *J Vac Sci Technol A* 15, 1319–1327 (1997)

Van Grieken R, Xhoffer C: Microanalysis of individual environmental particles. *J Anal Atomic Spec* 7, 81–88 (1992)

Wallace WE, Keane MJ: *Differential Surface Composition Analysis by Multiple-Voltrage Electron Beam X-Ray Microscopy*. U.S. Patent 5,210,414 (1993)

Wallace WE, Harrison J, Keane MJ, Bolsaitis P, Eppelsheimer D, Poston J, Page SJ: Clay occlusion of respirable quartz particles detected by low voltage scanning electron microscopy–x-ray analysis. *Ann Occup Hyg* 34, 195–204 (1990)

Wallace WE, Keane MJ, Harrison JC, Stephens JW, Brower PS, Grayson, RL, Attfield MD: Surface properties of silica in mixed dusts. In *Silica and Silica-Induced Lung Diseases* (Eds. Castranova V, Vallyathan V, Wallace WE). CRC Press, Boca Raton (1996) 107–117

Xhoffer C, Bernard P, Van Grieken RV, Van der Auwera L: Chemical characterization and source apportionment of individual aerosol particles over the North Sea and the English Channel using multivariate techniques. *Environ Sci Technol* 25, 1470–1478 (1991)